CHILEAN JOURNAL of AGRICULTURAL RESEARCH

CHILEANJAR CHILEAN JOURNAL of AGRICULTURAL RESEARCH

RESEARCH ARTICLE

Spatio-temporal changes of hydrothermal conditions and suitable habitat of *Citrus medica* L. var. sarcodactylis (Hoola van Nooten) Swingle in China under climate change

Yanli Xia[1], Yuxia Yang[2], Ting Li[1], Jian Ding[3], Ke Xu[4], Shiliang Xu[1], Yihe Wang[1], Xuchen Fan[1], Guofu Mei[5], Bo Yu[5], Jianming Yi[6], and Rulin Wang[7, 8*]

[1]Chengdu University, School of Food and Bioengineering, Chengdu 610106, PR China.
[2]Sichuan Provincial Key Laboratory of Quality and Innovation Research of Chinese Materia Medica, Sichuan Academy of Traditional Chinese Medicine Sciences, Chengdu 610041, PR China.
[3]Sichuan Science and Technology Exchange Center, Chengdu 610016, Sichuan, PR China.
[4]Sichuan Horticultural Crop Technology Extension Station, Chengdu 610041, Sichuan, PR China.
[5]Dazhou Dachuan Agricultural and Rural Bureau, Dazhou 635000, Sichuan, PR China.
[6]Guang 'an Cash Crop Technology Extension Station, Guang 'an 638500, Sichuan, PR China.
[7]Sichuan Provincial Rural Economic Information Center, Chengdu 610072, Sichuan, China.
[8]Water-Saving Agriculture in Southern Hill Area Key Laboratory of Sichuan Province, Chengdu 610066, Sichuan, PR China.
*Corresponding author (wrl_1986_1@163.com).
Received: 7 November 2022; Accepted: 11 January 2023, doi:10.4067/S0718-58392023000400380

ABSTRACT

Finger citron (*Citrus medica* L. var. *sarcodactylis* (Hoola van Nooten) Swingle; Rutaceae: *Citrus*) is an important plant for both medicine and food. Due to the lack of suitability analysis, many problems have arisen in its planting. According to the daily observation data, Kriging interpolation was selected to spatialize precipitation and temperature data. MaxEnt and ArcGIS were applied to simulate the suitable areas of finger citron in China from the perspectives of bioclimate, soil, topographic factors and human activities in 2050s and 2090s. Results showed that temperature annual range (Bio7), annual precipitation (Bio12), human footprint (Hf), elevation (El) and precipitation seasonality (Bio15) were identified as the dominant environmental variables related to the distribution of finger citron. Spatiotemporal distribution of annual precipitation (Bio12) showed that in the future, the precipitation in South China tends to decrease first (2050s) and then increase (2090s). The spatio-temporal analysis of temperature annual range (Bio7) showed that the 20-30 ℃ region was relatively stable in the Sichuan Basin and the middle and lower reaches of the Pearl River Basin. Under the future climate change scenarios, the total suitable area showed a significant increase trend in 2090s, and the change of most, moderately and poorly suitable habitats showed no obvious law. Under SSP1-2.6, SSP2-4.5 and SSP5-8.5 scenarios, the centroid of the most suitable habitat of finger citron would move to the northwest, southeast and southwest respectively. Our results can effectively carry out to promote the recovery of its population.

Key words: *Citrus medica* var. *sarcodactylis*, climate change, finger citron, hydrothermal conditions, MaxEnt, spatio-temporal changes, suitable habitat.

INTRODUCTION

Finger citron (*Citrus medica* L. var. *sarcodactylis* (Hoola van Nooten) Swingle; Rutaceae: *Citrus*) is an important plant for both medicine and food, which was first contained in the first traditional Chinese medicine treatise Shen Nong Ben Cao Jing (Figure 1). Some organs of citron can be incorporated into traditional Chinese medicine, i.e., root, stem, leaf, flower and fruit, and have unique functions of curing and preventing diseases, nourishing health and prolonging life (Zhao, 2012) (Figure 1C). According to ancient books, *C. medica* has the effects of rational gasification of phlegm, anti-emesis and anti-distension, soothing the liver and strengthening the spleen (Li et al., 2022). Modern scientific experiments have shown that finger citron has the effects of bacteriostasis, anti-inflammatory, anti-oxidation, anti-cancer cells, regulating the immune system (Peng et al., 2018). Finger citron is native to India and widely cultivated in France, Italy, Germany, USA and Southeast Asia (Zhang et al., 2018). In China, finger citron is cultivated in the south (Guangdong, Fujian, Chongqing, Sichuan and Zhejiang), especially in Jiangjin of Chongqing and Zhaoqing of Guangdong, which have the largest area and the highest yield (Zhao et al., 2020). Studies have shown that finger citron is not resistant to cold and drought, vulnerable to freezing damage (Zhang et al., 2018). Finger citron is often affected by diseases and insect pests, including citrus canker, citrus Huanglongbing, citrus anthracnose, *Panonychus citri* McGregor and *Phyllocnistis citrella* Stainton (Qing et al., 2020), as well as meteorological disasters such as high temperature, drought, and freezing (Bai et al., 2019) (Figures 1E, 1F).

Medicinal plant ecological regionalization is a systematic analysis and regional division of the distribution sites of traditional medicine growing in a specific environment, and is a common method for the suitability division of traditional medicine that is not clear about the potential planting areas (Sibeko et al., 2021). In recent years, the maximum entropy model (MaxEnt) has been applied to the study of habitat zoning of various medicinal plants under climate change scenarios since its good prediction ability. She et al. (2021) used MaxEnt to simulate the suitable distribution of the important medicinal resource plant *Notopterygium incisum* in the Three Rivers Headwater Region of China in the present and 2050s, and believed that the results would be conducive to the scientific protection and rational utilization of its resources. Dad and Rashid (2022) mapped the current and future geographical distributions of *Aconitum heterophyllum*, *Fritillaria cirrhosa*, *Meconopsis aculeata* and *Rheum webbianum* in Kashmir-Himalaya using MaxEnt. The above research proves that MaxEnt model can be well applied to the study of habitat suitability analysis of medicinal plants.

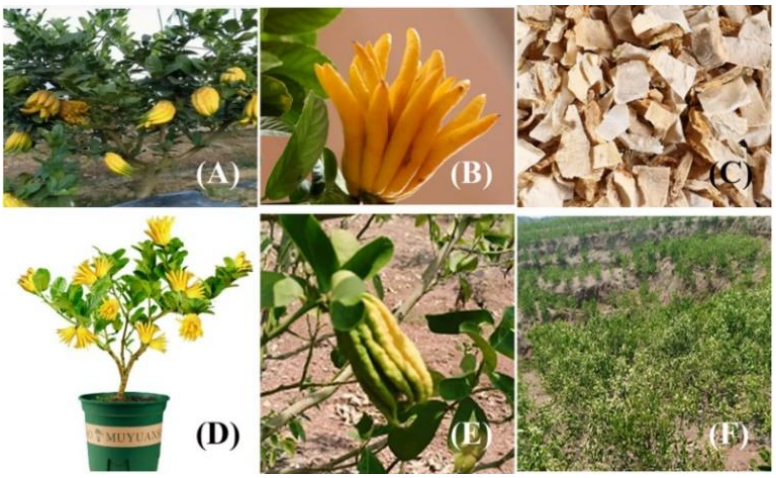

Figure 1. Field overview of *Citrus medica* var. *sarcodactylis* planting. A: Plant; B: fresh fruit; C: dried fruit slices; D: bonsai; E: fresh fruit under high temperature and drought; F: field under high temperature and drought.

The geographical distribution of plant species depends to a large extent on abiotic factors such as precipitation, temperature, soil and altitude, while climate factors are important conditions for plant growth, development and reproduction (Dad and Rashid, 2022). Studying the impact of climate change on crop distribution is conducive to the protection of germplasm resources and the sustainable development of ecological agriculture (Thudi et al., 2021; Vincent et al., 2022). The drastic change of climate will lead to the change of the original habitat of plants, and then affect their suitable range (Cheuk and Fischer, 2021; Liu et al., 2021). More and more scientific evidence shows that climate events such as climate warming, precipitation pattern change and atmospheric CO_2 concentration rise have made a significant influence on species diversity, genetic diversity and landscape diversity (Cobo-Simón et al., 2020). The formation of Chinese medicinal materials is closely related to the climate, and the climate change will certainly affect the changes of their distribution suitable areas (Sun and Zhang, 2015). Peng et al. (2013) found that due to the impact of climate change, the genuine producing areas of some medicinal materials in China have changed correspondingly, such as *Alisma orientale* and *Citrus aurantium*, while on the contrary, some have remained stable, such as *Chaenomeles speciosa* and *Fritillaria cirrhosa*.

Global climate change characterized by temperature rise and precipitation change is one of the great challenges facing mankind today, and has become an important factor affecting and restricting the sustainable development of natural systems, biological systems and human health systems (Ren et al., 2022). Climate change has greatly changed the spatial and temporal pattern of environmental factors, and agricultural production, which is heavily dependent on natural resources, shows obvious vulnerability in this context (Orrego-Verdugo et al., 2021). Temperature rise will increase the heat stress of most regions and crops in the world, and the instability of water stress due to precipitation fluctuation will pose a threat to crop production (Guzmán-Luna et al., 2022). The extreme weather events (rainstorm, flood, high temperature and drought disasters) caused by climate change have a direct impact on agricultural production, and then pose a huge challenge to people's growing demand and desire for a better life. Therefore, quantitative analysis of the spatio-temporal change trend and distribution characteristics of temperature and precipitation under climate change is of great significance to agricultural production and economic development (Abid et al., 2020). Gao et al. (2022) explored the crop phenology dynamics and climate response characteristics in the black soil region of Northeast China, and the result showed that 29.76% of the black soil region of Northeast China showed a significant delay in the onset of the growing season from 2000 to 2017. Teixeira et al. (2013) found through simulation that under the influence of changes in heat stress under the A1B emission scenario, the world's crop suitable areas will change from 2071 to 2100. Tang et al. (2016) calculated the spatial-temporal distribution of reference crop evapotranspiration in the Huang-Huai-Hai Plain under the main climate scenarios in the future, and their results provide basic data support for scientific allocation of agricultural water resources and scientific response to the impact of climate change on agricultural production. Research by Ling et al. (2019) shows that climate change will increase the heat resources in the rice growing season in China, reduce the radiation resources, and increase the heterogeneity of precipitation, which will significantly move the potential planting boundary of single and double cropping rice to the north.

So far, the research of finger citron has focused on physiologically active compounds and the quality of medicinal materials (Li et al., 2022), and no reports have been found on its suitable areas. In this paper, by analyzing the importance of modeling, the domain variables affecting the distribution of finger citron were screened and their spatio-temporal changes in current (1991-2020), 2050s (2041-2060), and 2090s (2081-2100) were analyzed. In addition, MaxEnt and ArcGIS were used to simulate the suitable areas of *C. medica* var. *sarcodactylis* in China from the perspectives of bioclimate, soil, topographic factors and human activities, and the climate change scenarios generated by global climate models (GCMs) were selected to predict its suitable areas in 2050s and 2090s, so as to master the impact of climate change on its planting suitability.

MATERIALS AND METHODS

Occurrence data of species

Occurrence data of Buddha's-hand or finger citron (*Citrus medica* L. var. *sarcodactylis* (Hoola van Nooten) Swingle) were acquired from the Global Biodiversity Information Facility (GBIF, https://www.gbif.org/), the Chinese Virtual Herbarium (CVH, https://www.cvh.ac.cn/), and literature. In addition, from 2018 to 2019, the research team conducted a field survey of some finger citron plantations in Zigong, Mianyang, Ya'an, Leshan, Bazhong, Nanchong, Luzhou and Yibin, Sichuan Province. We processed the distribution records of finger citron. Firstly, Baidu map picking coordinate system (Baidu, Beijing, PR China) was used to determine the longitude and latitude of records accurate to the town level. Second, Microsoft Excel (2010) was used to remove duplicate records. Third, the distance between each point and the center of the cell grid was calculated, and the point closest to the center in each cell grid was retained. After the above procedures, 123 records of finger citron were retained for the establishment of MaxEnt (Figure 2).

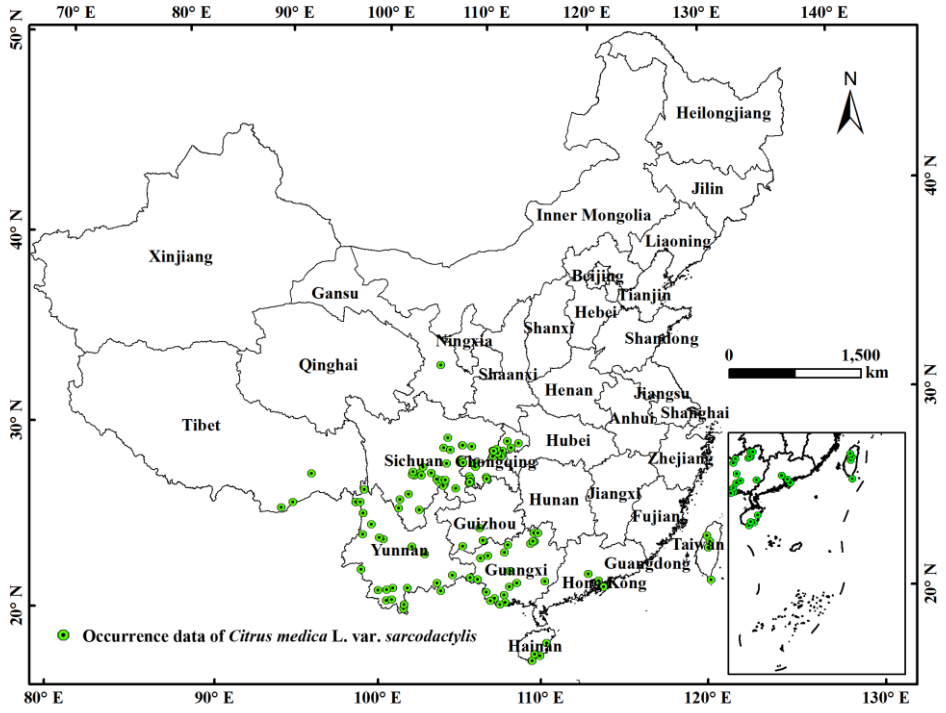

Figure 2. Occurrence data of *Citrus medica* var. *sarcodactylis*.

Environmental data

Twenty-seven initial environmental variables were selected in this study. In order to reduce the influence of multi-collinearity among 19 bioclimatic variables, Pearson correlation analysis method was used. Firstly, MaxEnt software version 3.4.4, developed by Phillips et al. (2006), was used to calculate the percent contribution of 19 environmental variables, and the variables whose percent contribution rate was greater than 0 were retained. Thereafter, the Pearson's coefficients between two variables with percent contribution greater than 0 corresponding to 123 occurrence data of finger citron were analyzed using SPSS (IBM, Armonk, New York, USA). Thirdly, by comparing the percentage contribution of the variables with the absolute value of the coefficient greater than 0.85, the higher one was retained. Finally, in addition to elevation, a total of 17 variables were selected to establish the prediction model of finger citron (Table 1).

Table 1. Environmental variables used to predict the potential geographic distribution of *Citrus medica* var. *sarcodactylis*. †Variable has no unit of measurement.

Code	Variable	Resolution	Unit
Bio1	Annual mean temperature	2.5'	℃
Bio2	Mean diurnal range	2.5'	℃
Bio5	Max temperature of warmest month	2.5'	℃
Bio7	Temperature annual range	2.5'	℃
Bio12	Annual precipitation	2.5'	mm
Bio15	Precipitation seasonality	2.5'	†
Bio17	Precipitation of driest quarter	2.5'	mm
El	Elevation	2.5'	m
Aspect	Aspect	2.5'	°
pH	Potential of hydrogen	2.5'	†
T-sand	Topsoil sand fraction	2.5'	%
T-C	Topsoil organic C	2.5'	%
Depth	Reference soil depth	2.5'	m
USDA	Topsoil USDA texture classification	2.5'	name
UV-B3	Mean UV-B of highest month	2.5'	kJ m^{-2}
Hf	Human footprint index	2.5'	†

Spatio-temporal analysis of hydrothermal conditions

According to the daily observation data of 824 meteorological stations in China from 1991 to 2020 provided by data set of China's surface climate data from the China Meteorological Data Service Centre (http://data.cma.cn/en), after excluding the daily average temperature and the missing measurement value of precipitation at 20-20 h, and converting snow, ice and fog into precipitation, the main bioclimatic variables were calculated. Based on the principle of geostatistics, Kriging method used the structure of sample data and variogram to estimate the unknown sample points of regionalized variables linearly, unbiased and optimally. According to previous studies, it was found that spatial interpolation of temperature based on Digital Elevation Model (DEM) can better simulate the spatial distribution of temperature data (Wild et al., 2022). Therefore, this paper used altitude as a covariate to perform ordinary Kriging interpolation on regional temperature indicators to spatialize temperature point data. As precipitation will be affected by many factors such as longitude, latitude, elevation, and slope direction, scholars believed that different interpolation methods should be selected according to the physical and geographical characteristics of the study area to establish an interpolation model (Bárdossy et al., 2021). Therefore, considering the complexity of the study area, the advantages of Kriging method and the consistency with this study method, ordinary Kriging interpolation is selected to spatialize precipitation data.

Modelling process

MaxEnt software operation procedure was as follows. 1) The occurrence data of finger citron in "CSV" format and the environmental variable in "ASC" format (including bioclimatic variables, elevation and human footprint) were imported into the "sample" and "environmental layers" data boxes of MaxEnt software respectively. 2) "Create response curves" and "Do jackknife to measure variable importance" were selected respectively to analyze the relationship between variables and presence probability of finger citron and measure the importance of variables. 3) In the initial model, "Random test percentage" was set to 25%, while in the reconstructed model, "random seed" was selected, and the "replicates" was set to 10. 4) Receiver operating characteristic (ROC) curve was selected to evaluate the models (Yang et al., 2022).

RESULTS AND DISCUSSION

Key environmental variables

Jackknife test showed that the regularized training gain of temperature annual range (Bio7) was the highest (1.47), and its percent contribution rate (18.25%) and permutation importance (39.68%) were at a higher level, indicating that it was one of the most important variables affecting the distribution of finger citron (Figures 3 and 4). The training gain and percent contribution of annual precipitation (Bio12) was 1.23 and 44.47%, indicating the importance of this variable. During the modeling of "without variables", the human footprint (Hf) had the largest decrease in the training gain value, indicating that it contains unique information related to the distribution of finger citron and has a great impact on its distribution (Figure 3). Through the above comprehensive comparison method, temperature annual range (Bio7), annual precipitation (Bio12), human footprint (Hf), elevation (El) and precipitation seasonality (Bio15) were identified as the dominant environmental variables related to the distribution of finger citron (Figures 3 and 4).

Environment is an important factor affecting the yield and quality of Chinese medicinal materials (Zhang et al., 2021). During the modeling of this study, in addition to the commonly used bioclimatic variables, terrain (elevation and aspect) and soil data (soil pH, topsoil sand fraction, topsoil organic C and reference soil depth) were also added. When predicting the impact of climate on the distribution of finger citron in the future, this study assumed that non climatic variables were unchanged. First, unlike the macro impact of climate, the impact of terrain, soil and other factors on plant distribution is limited to a relatively small range. Second, non-climatic variables, especially the change of terrain is a long-term and slow process, while a short time span of research generally defaults that the terrain factor is unchanged.

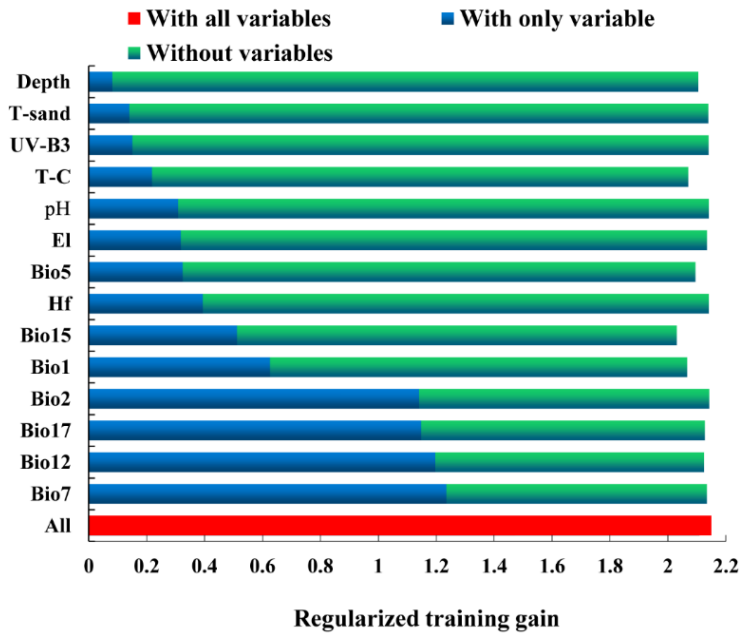

Figure 3. Jackknife test of 15 variables. Depth: Reference soil depth; T-sand: topsoil sand fraction; UV-B3: mean UV-B of highest month; T-C: topsoil organic C; El: elevation; Bio5: max temperature of warmest month; Hf: human footprint index; Bio15: precipitation seasonality; Bio1: annual mean temperature; Bio2: mean diurnal range; Bio17: precipitation of driest quarter; Bio12: annual precipitation; Bio7: temperature annual range.

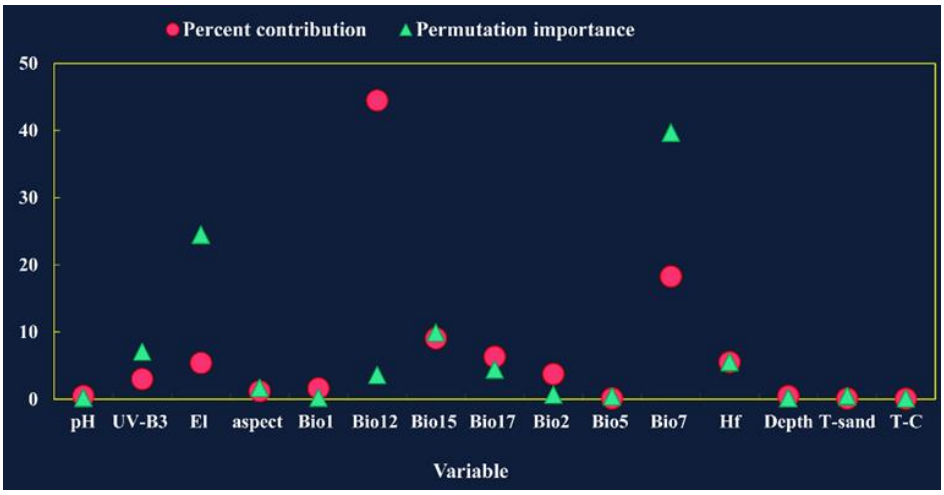

Figure 4. Percent contribution and permutation importance of 15 variables. UV-B3: Mean UV-B of highest month; El: elevation; Bio1: annual mean temperature; Bio12: annual precipitation; Bio15: precipitation seasonality; Bio17: precipitation of driest quarter; Bio2: mean diurnal range; Bio5: max temperature of warmest month; Bio7: temperature annual range; Hf: human footprint index; Depth: reference soil depth; T-sand: topsoil sand fraction; T-C: topsoil organic C.

Spatio-temporal changes of hydrothermal conditions

Spatio-temporal changes of the annual precipitation (Figure 5A) showed that under current climate situation, China's 300 mm isochore extends from the Daxing'an Mountains in the east of the Inner Mongolia Plateau to the Qilian Mountains in the north of the Loess Plateau and finally to the Himalayas in the west of the Qinghai Tibet Plateau. Under the three climate change scenarios, the position of the 300 mm isopotential line was relatively stable, but its northern section moved slightly westward (Figures 5B-5G).

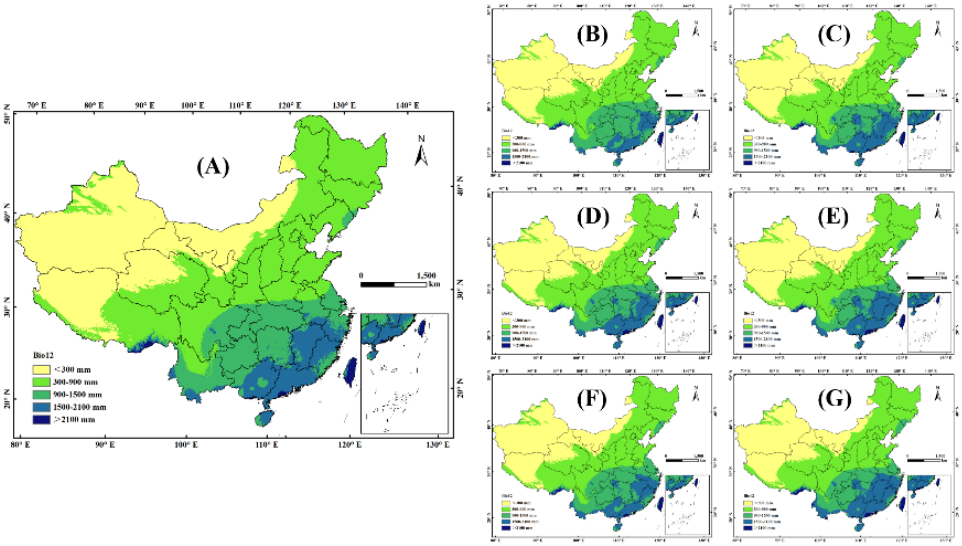

Figure 5. Spatio-temporal changes of the temperature annual range (Bio7). A: Current; B: 2050s, SSP1-2.6; C: 2090s, SSP1-2.6; D: 2050s, SSP2-4.5; E: 2090s, SSP2-4.5; F: 2050s, SSP5-8.5; G: 2090s, SSP5-8.5.

The 900 mm precipitation line starts from the Dabie Mountains in the East, passes through the Qinling Bashan mountains at the southern end of the Loess Plateau, and extends to the southern edge of the Hengduan Mountains in Southwest China (Figure 5A). Under SSP1-2.6, the western section of the isopotential line is relatively stable, while the eastern section expands northward in 2050s and contracts southward in 2070s. Under SSP2-4.5, the isopotential line changes obviously as a whole, first expanding northward in 2050s, and then contracting southward slightly in 2090s. Under SSP5-8.5, the position of the isopotential line changes most obviously. The western section gradually expanded northward from current to 2090s, especially in the northwest of Yunnan. The isochore along the Dabie Mountains in the eastern section first expanded northward in 2050s, and then contracted southward in 2090s (Figures 5B-5G).

The 1500 mm isopotential line starts from the southern end of the middle and lower reaches of the Yangtze River Plain in the East, passes through the Yunling mountains in the middle, and extends to the southern edge of the Xuefeng mountains in the West (Figure 5A). Under SSP1-2.6, the isopotential line will obviously retreat southward in 2050s, especially in the eastern section, which will be reduced from the current position to Wuyishan Mountain. In 2090s, the western section of the isopotential line will move northward slightly, the middle section will move to the vicinity of the Wushan mountains in a large scale, and the eastern section will shrink slightly. Under SSP2-4.5, the isopotential line will gradually move northward as a whole from contemporary to 2090s. Especially in 2090s, the middle section and east section will expand significantly to the north. Under SSP5-8.5, in 2050s, the western and eastern sections of the isopotential line will expand northward, while the middle section will retreat southward. By 2090s, the isopotential line will move significantly northward as a whole (Figures 5B-5G).

Spatio-temporal changes of the temperature annual range (Bio7) (Figure 6) shows the temporal and spatial changes of temperature annual range (Bio7) under three climate change scenarios from current to 2090s. Under current climate situation, regions with ＞ 50 ℃ are distributed in Northeast and Northwest China. In the northeast, it is mainly located in the north central part of the Northeast Plain, Xiaoxing'an Mountains and Daxing'an Mountains. In the northwest, it is mainly located in Tarim Basin and Junggar basin (Figure 6A). Under SSP1-2.6 and SSP2-4.5, regions with ＞ 50 ℃ is gradually decreasing, and the reduced area is mainly located in the south of the Northeast Plain and the east of the Tarim Basin, while the reduction range is larger under SSP2-4.5. Under SSP5-8.5, the area > 50 ℃ first shrank significantly in 2050s, and then expanded slightly in 2090s (Figures 6B-6G).

Under current climate situation, the 40-50 ℃ region is located in the south of the Northeast Plain, the Inner Mongolia Plateau, the north of the Loess Plateau and the north of the Qinghai Tibet Plateau (Figure 6A). Under the three climate change scenarios, it will move northward as a whole respectively (Figures 6B-6G).

Under current climate situation, the 40 ℃ isotherm starts from Liaodong Peninsula in the east, passes through the North China Plain, the Loess Plateau, the Qilian Mountains, and reaches the Kunlun Mountains in the West (Figure 6A). Under SSP1-2.6, SSP2-4.5 and SSP5-8.5, the isotherm will move northward as a whole. The east section of the northern boundary will extend northward to the north of Liaodong Peninsula, and the middle section will move out of the North China Plain (Figures 6B-6G).

Under current climate condition, the eastern section of the 30 ℃ isotherm is distributed along Wuyishan-Yunling Mountain, the middle section is distributed along Wushan Mountain from north to south, and the western section is from Qinling-Bashan Mountain to the eastern margin of Himalayas through Hengduan Mountain (Figure 6A). Under SSP1-2.6, the western section of the 30 ℃ isotherm will not change much in the future, while the eastern section will retreat slightly to the south in 2050s, but move significantly northward to the north of the Huaihe River in 2090s. Under SSP2-4.5, the western section of the isotherm will not change much in the future, while the eastern section will move northward from the Yangtze River basin to the Huaihe River in the 2050s, but will retreat slightly southward in the 2090s. Under SSP5-8.5, the eastern section will first expand slightly northward in 2050s, and then contract slightly southward in 2090s (Figures 6B-6G).

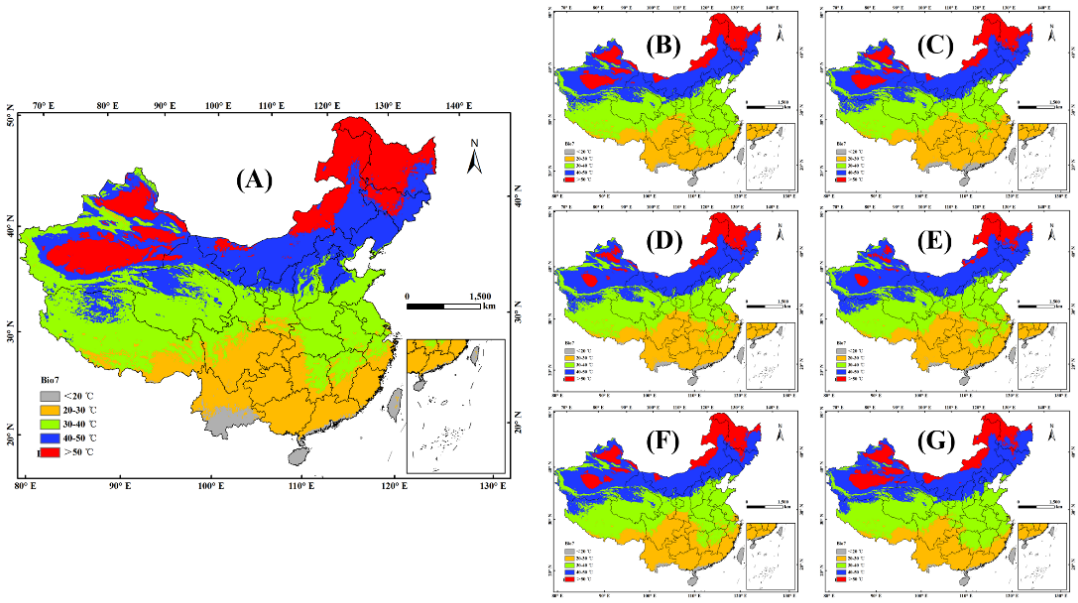

Figure 6. Spatio-temporal changes of the annual precipitation (Bio12). A: Current; B: 2050s, SSP1-2.6; C: 2090s, SSP1-2.6; D: 2050s, SSP2-4.5; E: 2090s, SSP2-4.5; F: 2050s, SSP5-8.5; G: 2090s, SSP5-8.5.

Under the current climate condition, the 20 ℃ isotherm is divided into two sections, the western section is located on the south side of the Yunnan-Guizhou Plateau, and the eastern section is located on the southern coast of Guangdong (Figure 6A). Under SSP1-2.6, the western section will retreat southward to the edge of Yunnan Guizhou Plateau in 2050s, and then move northward slightly in 2090s. The eastern section will gradually expand northward from current to 2090s (Figures 6B-6G).

The spatio-temporal analysis of temperature annual range (Bio7) showed that the 20-30 ℃ region was relatively stable in the Sichuan Basin and the middle and lower reaches of the Pearl River Basin, which is the distribution area of the suitable growth area of finger citron. Widrlechner et al. (2012) used the annual average minimum temperature as an index to draw the Plant Hardiness Zone Map (PHZM) in China, and divided it into 11 grades. Combined with our result, the distribution range of finger citron was located in grade 9-11 (-6.6 ~ 4.5 ℃). Therefore, only from the perspective of adaptability to temperature variables, finger citron was almost suitable for planting in most areas south of 31° N in China.

Suitable habitat under current climate condition

After reclassification and format conversion of the results output by MaxEnt, the area calculated by ArcGIS showed that the total suitable area of finger citron in China was 177.36×10^4 km^2, accounting for 18.47% of the total area of the country, of which the distribution range of the most suitable habitat was the narrowest, with an area of 22.27×10^4 km^2, accounting for 12.55% of the total suitable habitat. Figure 7 showed that the most suitable habitat was located in the middle east of Sichuan, western Chongqing in the upstream of the Yangtze River and western Taiwan, southern Guizhou and western Guangxi in the upstream of the Pearl River, central and southern Yunnan and Southeast Tibet in the Middle-Lower reaches of the Southwest River. The moderate suitable habitat extended to the periphery along the most suitable habitat, with an area of 51.96×10^4 km^2, accounting for 29.3% of the total suitable habitat, mainly distributed in northeast Sichuan, central Chongqing and northern Guizhou in the upper reaches of the Yangtze River Basin, most of Guangxi in the upper reaches of the Pearl River Basin and central Guangdong in the lower reaches, southern Yunnan in the lower reaches of the Southwest River basin and most of Hainan (Figure 7). The poorly suitable habitat

of finger citron were mainly distributed in the northeast and south of Sichuan, north of Chongqing, south of Shaanxi, west of Hubei, west of Hunan, northeast and northwest of Guizhou in the middle and upper reaches of the Yangtze River Basin, east of Jiangxi in the lower reaches of the Yangtze River, most of Fujian in the southeast River Basin, most of Guangxi in the upper reaches of the Pearl River Basin and Guangdong in the lower reaches, southeast of Tibet and north central Yunnan in the lower reaches of the Southwest River basin, covering an area of 103.13×10^4 km^2, accounting for 58.15% of the total suitable habitat (Figure 7).

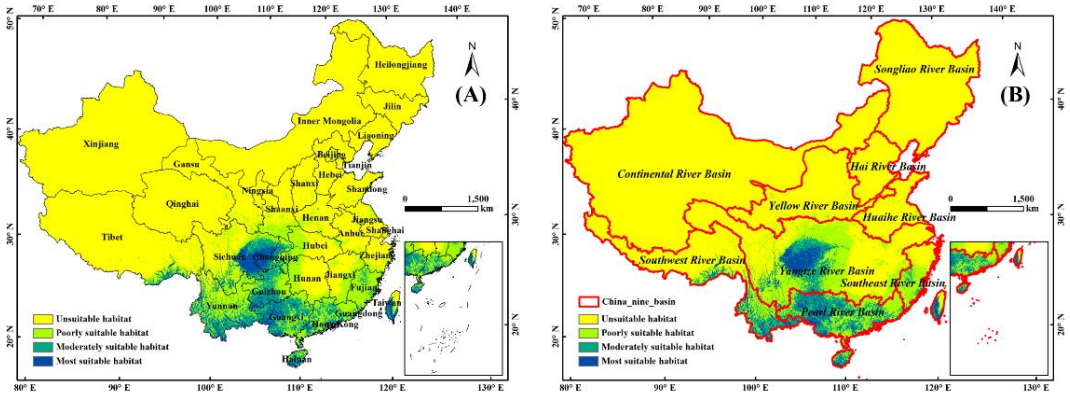

Figure 7. Suitable habitat simulated based on administrative division (A) and watershed division (B) by MaxEnt under current climate situation.

Finger citron is native to India, mainly cultivated in China, with few wild species. With the cultivation and introduction, finger citron has been widely planted in Sihui, Chaoshan, Yunfu and Yunan of Guangdong, Tianlin, Longlin, Lingle, Guanyang, Daxin and Yongfu of Guangxi, Kunming, Yuxi, Chuxiong, Xinping, Yimen, Eshan and Pu'er of Yunnan, Jiangjin, Yongchuan, Yunyang and Kai counties of Chongqing, Anxian, Hejiang, Yibin, Muchuan, Ya'an, Hongya, Jiajiang, Qianwei and Xingjing of Sichuan (Zhao et al., 2020). Our simulation showed that the most suitable habitats were distributed in the middle east of Sichuan, western Chongqing, southern Guizhou and western Guangxi, central and southern Yunnan and southeast Tibet, with an area of 22.27×10^4 km^2. The actual production area has a high degree of overlap with our simulation, indicating the accuracy of MaxEnt. According to the data, the actual planting area of finger citron is far smaller than its suitable area, which may be limited by the selected variables. In this study, we simulated the suitable habitat of finger citron under the combination of dominant natural environmental variables, and does not involve production management and the impact on fruit yield and quality. In the actual production of finger citron, social and economic factors such as labor force, field management, production cost and market demand are also important drivers affecting its planting, which makes our prediction area far higher than its actual production area. In addition, due to the need to simulation the distribution of finger citron in the future, there is no corresponding prediction model for socio-economic variables at present, which is also the reason that affects our choice of variables.

Suitable habitat in the future

Under SSP1-2.6, the areas of the most suitable habitats were 22.27×10^4 km^2 (2050s) and 22.12×10^4 km^2 (2090s), reducing by 4.85% and 0.65% compared with current situation, respectively. The areas of moderately suitable habitats were 47.08×10^4 km^2 (2050s) and 56.21×10^4 km^2 (2090s), which were decreased by 9.4% (2050s) and increased by 8.17% (2090s) compared with current. The areas of poorly suitable habitats were 106.11×10^4 km^2 (2050s) and 108.86×10^4 km^2 (2090s), which were increased by 2.89% (2050s) and 5.55% (2090s) compared with current respectively. The area of total suitable habitats was 174.38×104 km^2 (2050s) and 187.19×104 km^2 (2090s), which were decreased by 1.68% (2050s) and increased by 5.54% (2090s) compared with current, respectively (Figures 8A-8B, 9).

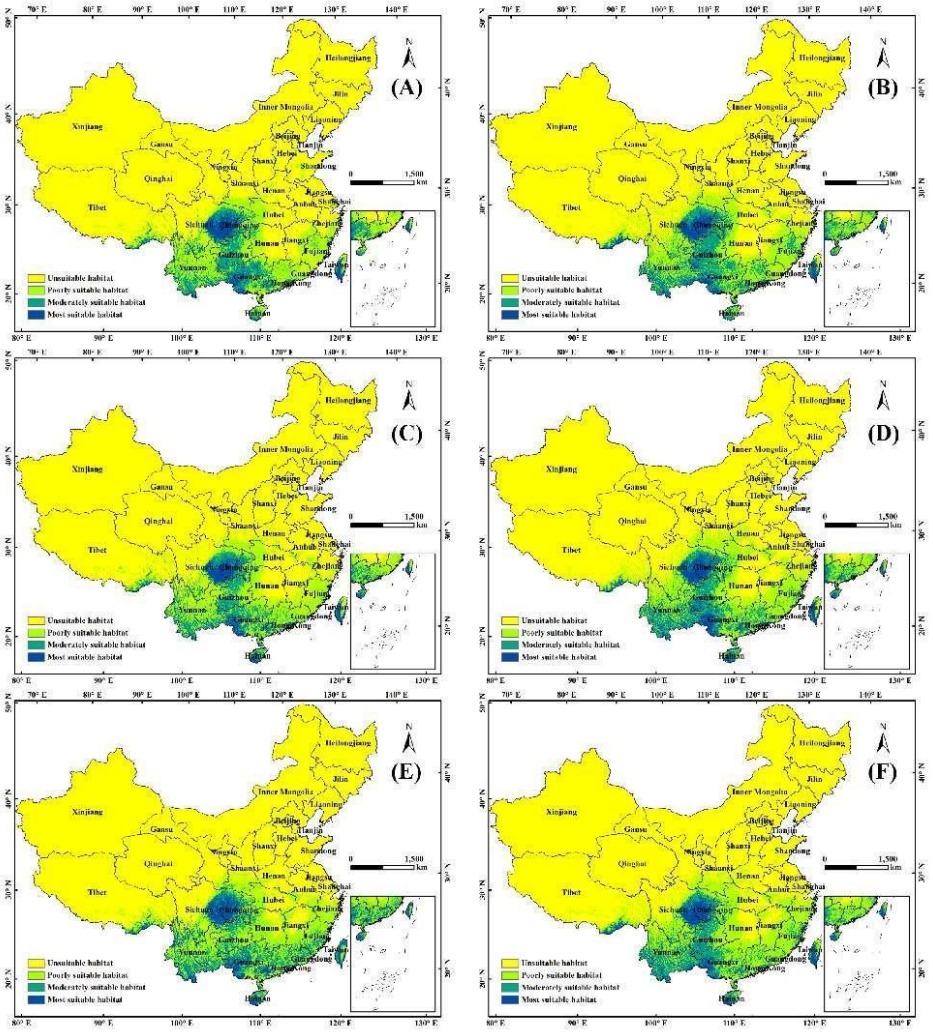

Figure 8. Suitable habitat simulated by MaxEnt under climate change scenarios. A: 2050s, SSP1-2.6; B: 2090s, SSP1-2.6; C: 2050s, SSP2-4.5; D: 2090s, SSP2-4.5; E: 2050s, SSP5-8.5; F: 2090s, SSP5-8.5.

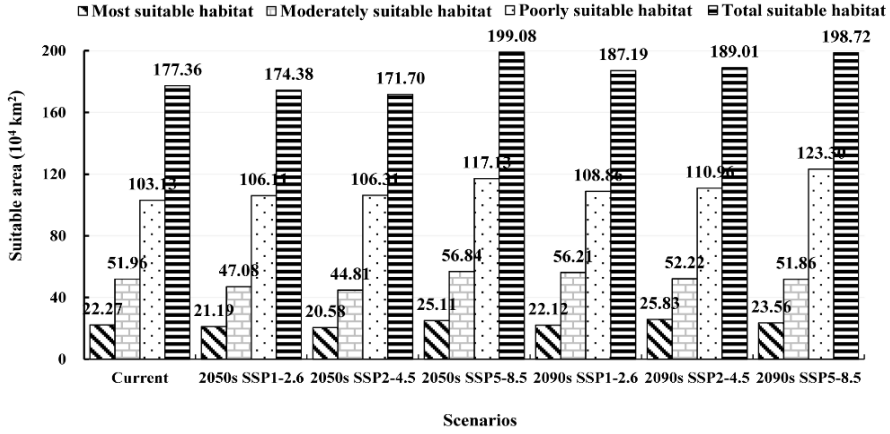

Figure 9. Areas of suitable habitat under climate change scenarios.

Under SSP2-4.5, the areas of highly suitable habitats were 20.58×10^4 km^2 (2050s) and 25.83×10^4 km^2 (2090s), which were decreased by 7.56% (2050s) and increased by 16% (2090s) compared with current, respectively. The areas of moderately suitable habitats were 44.81×10^4 km^2 (2050s) and 52.22×10^4 km^2 (2090s), which were decreased by 13.77% (2050s) and increased by 0.5% (2090s) compared with current, respectively. The areas of poorly suitable habitats were 106.31×10^4 km^2 (2050s) and 110.96×10^4 km^2 (2090s), which were increased by 3.08% (2050s) and 7.59% (2090s) compared with current, respectively. The areas of total suitable habitats were 171.7×10^4 km^2 (2050s) and 189.01×10^4 km^2 (2090s), which were decreased by 3.19% (2050s) and increased by 6.57% (2090s) compared with current respectively (Figures 8C-8D, 9).

Under SSP5-8.5, the areas of highly suitable habitats were 25.11×10^4 km^2 (2050s) and 23.56×10^4 km^2 (2090s), which were increased by 12.79% (2050s) and 15.83% (2090s) compared with current respectively. The areas of moderately suitable habitats were 56.84×10^4 km^2 (2050s) and 51.86×10^4 km^2 (2090s), which were increased by 9.38% (2050s) and decreased by 0.2% (2090s) compared with current respectively. The areas of poorly suitable habitats were 117.13×10^4 km^2 (2050s) and 123.3×10^4 km^2 (2090s), which were increased by 13.57% (2050s) and 19.55% (2090s) compared with current respectively. The areas of total suitable habitat were 199.08×10^4 km^2 (2050s) and 198.72×10^4 km^2 (2090s), which were increased by 12.25% (2050s) and 12.04% (2090s) compared with current respectively (Figures 8E-8F, 9).

Climate change will lead to changes in the future geographical distribution pattern of species, aggravate the reduction of biodiversity and the loss of germplasm resources, and accelerate the extinction rate of species. Therefore, it is very important for species protection and sustainable utilization of resources to carry out research on the distribution pattern and change of species' suitable habitat under the background of climate change and to understand the characteristics and change trend of species' future geographical distribution pattern. Studying the relationship between plant climate demand and geographical distribution and understanding the response of plant distribution pattern to climate change is of great significance to put forward reasonable utilization strategies and planting zoning, and to reveal the history of species formation, migration and diffusion (Ardestani and Ghahfarrokhi, 2021). Global climate change is an important driving factor to change the geographical distribution pattern of species (Nascimbene et al., 2020). The impact of climate change on species has two sides, that is, some species will benefit from it, and their distribution will expand, while the habitat of other species will decrease (Ribeiro-Souza et al., 2022). In this paper, we found that under the SSP1-2.6 and SSP2-4.5 in 2050s, the total suitable area of finger citron changed slightly, while under other scenarios, the area increased significantly. This change trend indicated that the future climate change would be favorable to finger citron as a whole, and such expending trend had also been found in other medicinal plants. Zhao et al. (2021) found that climate change caused the expansion of the suitable habitat area of Tibetan medicine *Lamiophlomis rotata* to be about twice of the degraded area, and the area in all provinces showed an increasing trend. Xu et al. (2022) predicted the distribution of *Thesium chinense* in China, and their results revealed that the area of the highly suitable area would increase gradually and expanded from the Yangtze River basin to the Yellow River Basin. The higher precipitation under the high concentration emission scenario can reduce the restriction of precipitation factors on the distribution of species and expand the suitable habitat of species. On the contrary, the increased precipitation under the low concentration emission scenario cannot reduce the limit, but will reduce the available water for species to absorb with global warming (Peltonen-Sainio et al., 2021; Liu et al., 2022; Ren et al., 2022). This is consistent with the change law of the total suitable habitat of finger citron under climate change. Based on the above analysis, we speculated that the reduction of the total suitable habitat of finger citron in 2050s may be due to the excessive drought caused by the temperature rise, while the increase of the suitable habitat in 2090s may be related to the gradual accumulation of rainfall.

Trajectory and change trend of centroid of the most suitable habitat

Under different time periods and climate change scenarios, the change trend of species' suitable habitat can be quantitatively described by calculating the position of the centroid. The movement trajectory and change trend of finger citron were revealed as follows. 1) Under SSP1-2.6, the centroid would move 64.27 km from

105.9°E/26.68°N (current) to the northeast to 106.22°E/27.23°N (2050s), and then 61.8 km to the southwest to 105.73°E/26.86°N (2090s). From current to 2090s, the centroid would generally move 24.97 km to the northwest (Figure 10). 2) Under SSP2-4.5, the centroid would move 57.43 km from 105.9°E/26.68°N (current) to the southeast to 106.47°E/26.63°N (2050s), and then 35.64 km to the southwest to 106.34°E/26.3°N (2090s). From current to 2090s, the centroid would generally move 57.89 km to the southeast (Figure 10). 3) Under SSP5-8.5, the centroid would move 19.23 km from 105.9°E/26.68°N (current) to the northeast to 106.09°E/26.7°N (2050s), and then 35.1 km to the southwest to 105.74°E/26.66°N (2090s). From current to 2090s, the centroid would generally move 15.88 km to the southwest (Figure 10).

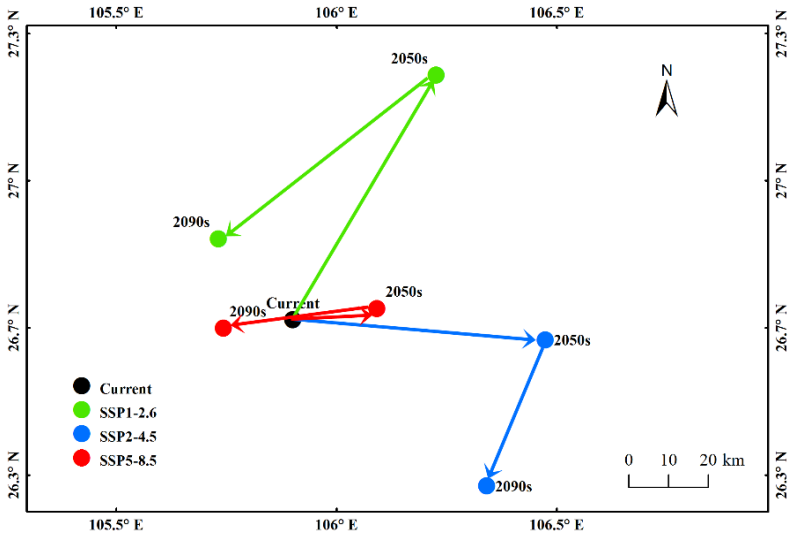

Figure 10. Trajectory trend of centroid of the most suitable habitat.

From current to 2090s, the centroid of the most suitable habitat of finger citron would move to the northwest (SSP1-2.6), southeast (SSP2-4.5) and southwest (SSP5-8.5), respectively, which indicated that the impact of climate change on its distribution was uncertain, and changes in temperature and precipitation under different scenarios may be the cause of this phenomenon. Xiang et al. (2021) found through simulation that under SSP1-2.6 scenario, the increasing trend of temperature rise rate and extreme precipitation rate in China from 2021 to 2100 was relatively flat, while under SSP2-4.5, SSP3-7.0 and SSP5-8.5 scenarios, they gradually increase with the increase of mode and time.

The global population and economic level have gained rapid growth since the 20th century, and human activities have had a great impact on the living environment (Tischer et al., 2022). Climate change and human activities are considered to be the leading factors affecting the structure and function of terrestrial ecosystems (Zhai et al., 2020). Importance analysis showed that human footprint was the key variable affecting the distribution of finger citron, and the appropriate range was ≥ 6.99. Finger citron is mostly cultivated in China, and the impact of agricultural activities on its distribution cannot be ignored. Cutting, grafting and high-pressure propagation are the main propagation methods of finger citron (Peng et al., 2018). With the continuous optimization of China's agricultural industrialization, the continuous adjustment of agricultural planting structure, and the government's regulation on the market, the planting area of finger citron has expanded in Sichuan and Chongqing. On the contrary, Yue et al. (2018) investigated the resources of finger citron in Guangdong, and found that due to the influence of production technology, market conditions and economic benefits, the planting area of finger citron in Guangdong was shrinking year by

year. All these prove the importance of human activities to the cultivation and distribution of finger citron, and this factor cannot be ignored in its planting planning.

Relationship between key environmental variables and presence probability of *C. medica* var. *sarcodactylis*

When the annual precipitation (Bio12) was 1311.72 mm, the presence probability of finger citron reached the peak and then decreased gradually (Figure 11A). Temperature annual range (Bio7) had a negative impact on the presence probability of finger citron, that was, with the increase of Bio7, the probability showed a downward trend (Figure 11B). When the elevation (El) < 347.12 m, it had a positive impact on the presence probability of finger citron, that was, the existence probability increased with elevation, while when the elevation > 347.12 m, it had a negative impact on the presence probability (Figure 11C). With the increase of human footprint, the presence probability of finger citron showed an upward trend, and the two were basically positively correlated (Figure 11D).

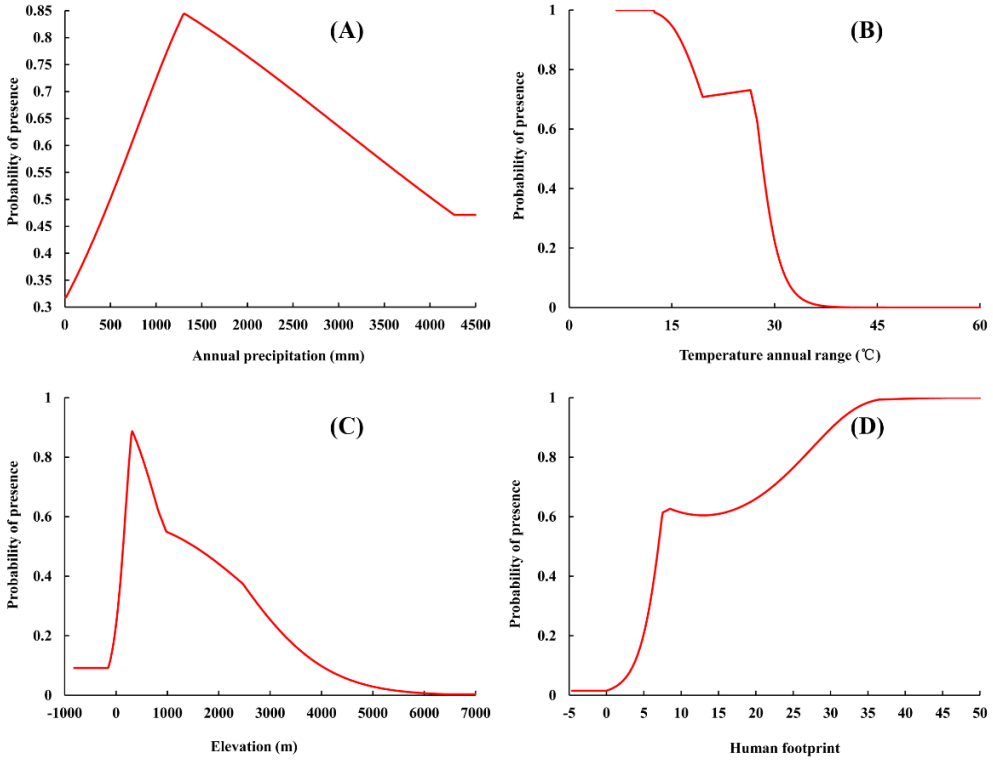

Figure 11. Response curves of dominant variables.

As a tropical and subtropical plant, finger citron likes a warm, humid and sunny environment, is not resistant to severe cold, and is suitable for cultivation in areas with sufficient rainfall and no freezing in winter (Zhao, 2012; Zhang et al., 2018; Li et al., 2022). Response curves showed that the variables proper for the existence of finger citron and their ranges were temperature annual range (< 28.07 ℃), annual precipitation (> 964.67 mm), which were similar to their growth habits. Importance analysis showed that temperature annual range (Bio7) was a domain temperature variable affecting the geographical distribution pattern of finger citron. When temperature annual range (Bio7) was higher than 28.07 ℃, the presence probability of finger citron decreased rapidly, indicating that too large temperature difference was not conducive for its survival. The spatio-temporal analysis of temperature annual range (Bio7) showed that the 20-30 ℃ region was relatively stable in the Sichuan

Basin and the middle and lower reaches of the Pearl River Basin, which is the distribution area of the suitable growth area of finger citron. Scholars pointed out that temperature restricts the distribution of plants in latitude, and precipitation is an important factor that affects the changes of plants from coastal to inland, which together restrict the geographical distribution pattern of plants (Jafarian et al., 2019). Response curve showed that the annual precipitation suitable for the existence of finger citron needs to be higher than 964.67 mm. Citrus plants need 300-500 parts of water for each part of DM formed in photosynthesis, and this genus requires a large amount of water (Ortuño et al., 2009). The annual precipitation suitable for citrus cultivation is 1000-1500 mm, while in the area with annual precipitation of 200 ~ 600 mm, in order to achieve high and stable yield of citrus, it is necessary to supplement water equivalent to 800 ~ 900 mm rainfall (Tu et al., 2021). Under the background of global climate change, the annual average temperature in China has increased by 0.4 ~ 0.5 ℃ in the past 100 yr, and the precipitation has shown obvious regional characteristics (Tan et al., 2010). Specifically, South China shows a warm and humid trend as a whole, and the whole South shows a tendency of being drier in the northwest and wetter in the southeast (Tan et al., 2010). Our spatio-temporal distribution of annual precipitation (Bio12) showed that under the three climate change scenarios, the precipitation in South China tends to decrease first (2050s) and then increase (2090s), and in Southwest China was generally stable. Combined with the simulation results, we believe that the precipitation in the suitable habitat will remain relatively stable under climate change, which provides ideal conditions for its planting. The above suggested that for the division of finger citron planting, in addition to temperature, whether the local precipitation and irrigation conditions could meet the above requirements should also be paid attention to.

Evaluation of models

Table 2 showed that the AUC (area under receiver operating characteristic curve) values of the training data and test data of the MaxEnt model under current situation were 0.969 ± 0.001 and 0.952 ± 0.013 respectively. The AUC values of the training data of the future climate scenario models were 0.963 ± 0.002-0.969 ± 0.002 and that of the test data were 0.945 ± 0.014-0.955 ± 0.018.

Table 2. Area under receiver operating characteristic curve (AUC) values of models.

Period	Scenario	Training data	Test data
Current (1991-2020)		0.969 ± 0.001	0.952 ± 0.013
2050s (2041-2060)	SSP1-2.6	0.969 ± 0.002	0.950 ± 0.016
	SSP2-4.5	0.969 ± 0.002	0.955 ± 0.018
	SSP5-8.5	0.964 ± 0.001	0.948 ± 0.019
2090s (2081-2100)	SSP1-2.6	0.965 ± 0.002	0.948 ± 0.025
	SSP2-4.5	0.965 ± 0.002	0.950 ± 0.017
	SSP5-8.5	0.963 ± 0.002	0.945 ± 0.014

CONCLUSIONS

According to the above prediction results, the protection and breeding of wild germplasm resources of *Citrus medica* var. *sarcodactylis* can be effectively carried out to promote the recovery of its population. At the same time, as a commonly used medicinal material in China, the introduction and cultivation of *C. medica* var. *sarcodactylis* in various suitable habitats will alleviate the imbalance between the shrinking supply of wild resources and the increase of market demand. In addition to the traditional production areas, the site selection range can be reasonably planned according to the dominant environmental factors affecting the

distribution of *C. medica* var. *sarcodactylis* and the change trend of future suitable areas, so as to improve the quality and output and promote industrial development.

Author contributions

Conceptualization: Y.L.X., Y.X.Y. Methodology: R.L.W. Software: T.L., J.D. Validation: K.X. Formal analysis: S.L.X. Investigation: Y.H.W., X.C.F. Resources: G.F.M., B.Y. Data curation: J.M.Y. Writing-original draft: Y.L.X., R.L.W. Writing-review & editing: Y.X.Y. Visualization: Y.X.Y. Supervision: Y.L.X. Project administration: Y.L.X., R.L.W. Funding acquisition: Y.L.X., R.L.W. All co-authors reviewed the final version and approved the manuscript before submission.

Acknowledgements

This work was funded by the Natural Science Foundation of Sichuan Province (2022NSFSC0589), the Sichuan Genuine Medicinal Materials and Traditional Chinese Medicine Innovation Team (SCCXTD-2022-19), the Sichuan Science and Technology Program (2021YFYZ0012, 2020YJ0359), the Key R & D projects of the Science and Technology Deportment of Sichuan Province (2022YFS0592), and the Heavy Rain and Drought-Flood Disasters in Plateau and Basin Key Laboratory of Sichuan Province (SCQXKJYJXZD202209).

References

Abid, M., Ali, A., Rahut, D.B., Raza, M., Mehdi, M. 2020. Ex-ante and ex-post coping strategies for climatic shocks and adaptation determinants in rural Malawi. Climate Risk Management 27:100200.

Ardestani, E.G., Ghahfarrokhi, Z.H. 2021. Ensembpecies distribution modeling of Salvia hydrangea under future climate change scenarios in Central Zagros Mountains, Iran. Global Ecology and Conservation 26:e01488.

Bai, Q.F., Huo, Z.G., Wang, J.H., Zhang, Y. 2019. Progress in research on meteorological disaster indicators of major fruit trees in China. Journal of Fruit Science 36:1229-1243.

Bárdossy, A., Modiri, E., Anwar, F., Pegram, G. 2021. Gridded daily precipitation data for Iran: A comparison of different methods. Journal of Hydrology: Regional Studies 38:100958.

Cheuk, M.L., Fischer, G.A. 2021. The impact of climate change on the distribution of *Castanopsis* (Fagaceae) species in south China and Indo-China region. Global Ecology and Conservation 26:e01388.

Cobo-Simón, I., Méndez-Cea, B., Jump, A.S., Seco, J., Gallego, F.J., Linares, J.C. 2020. Understanding genetic diversity of relict forests. Linking long-term isolation legacies and current habitat fragmentation in *Abies pinsapo* Boiss. Forest Ecology and Management 461:117947.

Dad, J., Rashid, I. 2022. Differential responses of Kashmir Himalayan threatened medicinal plants to anticipated climate change. Environmental Conservation 49:33-41.

Gao, J.B., Liu, L.L., Guo, L.H., Sun, D.Q., Liu, W.L., Hou, W.J., et al. 2022. Synergic effects of climate change and phenological variation on agricultural production and its risk pattern in black soil region of Northeast China. Acta Geographica Sinica 77:1681-1700.

Guzmán-Luna, P., Mauricio-Iglesias, M., Flysjö, A., Hospido, A. 2022. Analysing the interaction between the dairy sector and climate change from a life cycle perspective: A review. Trends in Food Science and Technology 126:168-179.

Jafarian, Z., Kargar, M., Bahreini, Z. 2019. Which spatial distribution model best predicts the occurrence of dominant species in semi-arid rangeland of northern Iran? Ecological Informatics 50:33-42.

Li, C.Y., Yuan, Z., She, C.J., Bi, J.Y. 2022. Research progress on chemical constituents and pharmacological actions of Citri sarcodactylis Fructus. Food and Drug 24:187-193.

Ling, X.X., Zhang, Z.L., Zhai, J.Q., Ye, S.C., Huang, J.L. 2019. A review for impacts of climate change on rice production in China. Acta Agronomica Sinica 45:323-334.

Liu, X., Lai, Q., Yin, S., Bao, Y., Qing, S., Bayarsaikhan, S., et al. 2022. Exploring grassland ecosystem water use efficiency using indicators of precipitation and soil moisture across the Mongolian Plateau. Ecological Indicators 142:109207.

Liu, L., Wang, R.L., Zhang, Y.Y., Mou, Q.Y., Gou, Y.S., Liu, K., et al. 2021. Simulation of potential suitable distribution of *Alnus cremastogyne* Burk. In China under climate change scenarios. Ecological Indicators 133:108396.

Nascimbene, J., Benesperi, R., Casazza, G., Chiarucci, A., Giordani, P. 2020. Range shifts of native and invasive trees exacerbate the impact of climate change on epiphyte distribution: The case of lung lichen and black locust in Italy. Science of the Total Environment 735:139537.

Orrego-Verdugo, R., Abarca-del-Rio, R., Lara-Uribe, C. 2021. Spatial dynamics and consistency of agroclimatic trends in Chile during 1985-2015 to the Köppen-Geiger climate classification. Chilean Journal of Agricultural Research 8:618-629.

Ortuño, M.F., García-Orellana, Y., Conejero, W., Pérez-Sarmiento, F., Torrecillas, A. 2009. Assessment of maximum daily trunk shrinkage signal intensity threshold values for deficit irrigation in lemon trees. Agricultural Water Management 96:80-86.
Peltonen-Sainio, P., Juvonen, J., Korhonen, N., Parkkila, P., Sorvali, J., Gregow, H. 2021. Climate change, precipitation shifts and early summer drought: An irrigation tipping point for Finnish farmers? Climate Risk Management 33:100334.
Peng, H.S., Hao, J.D., Huang, L.Q. 2013. Effect of climate change on genuine medicinal materials producing areas during last 2000 years—*Alisma orientale* and *Citrus aurtantium* as examples. China Journal of Chinese Materia Medica 38:2218-2222.
Peng, B., Wen, Y., Yu, R.M., Zhu, J.H. 2018. Advances in extraction, structure characterization and bioactivities of *Citrus medica* polysaccharide. Food and Drug 20:236-240.
Phillips S.J., Anderson R.P., Schapire R.E. 2006. Maximum entropy modeling of species geographic distributions. Ecological Modelling 190:231-259.
Qing, L.S., Zeng, J., Tong, W., Sun, P., Hu, L.S., Wu, F.M., et al. 2020. The historical evolution and cultivation technology of the medicinal and edible plant *Citrus medica* var. *sarcodactylis*. Journal of Agriculture 10:82-87.
Ren, S., Chen, X., Pan, C. 2022. Temperature-precipitation background affects spatial heterogeneity of spring phenology responses to climate change in northern grasslands (30°N-55°N). Agricultural and Forest Meteorology 315:108816.
Ribeiro-Souza, P., Graipel, M.E., Astúa, D., Vancine, M.H., Pires, J.S.R. 2022. Effects of climate change on distribution and areas that protect two neotropical marsupials associated with aquatic environments. Ecological Informatics 68:101570.
She, Y.D., Zhou, H.K., Zhang, Z.H., Ma, L., Zhou, B.R., Song, M.H., et al. 2021. Suitable distribution of *Notopterygium incisum* in the Three Rivers Headwater region under climate change. Ecology and Environment Sciences 30:2033-2041.
Sibeko, L., Johns, T., Cordeiro, L.S. 2021. Traditional plant use during lactation and postpartum recovery: Infant development and maternal health roles. Journal of Ethnopharmacology 279:114377.
Sun, M., Zhang, Z.L. 2015. Research progress in medicinal plants response to climate change. Journal of Biology 32:84-88.
Tan, K., Yu, Y., Zhang, T., Fang, J., Piao, S., Ciais, P., et al. 2010. The impacts of climate change on water resources and agriculture in China. Nature 467:43-51.
Tang, X.P., Song, N., Chen, Z.F., Wang, J.L. 2016. Spatial and temporal distribution of ET_0 under main climate scenarios in future across Huang-Huai-Hai Plain. Transactions of the Chinese Society of Agricultural Engineering 32(14):168-176.
Teixeira, E.I., Fischer, G., van Velthuizen, H., Walter, C., Ewert, F. 2013. Global hot-spots of heat stress on agricultural crops due to climate change. Agricultural and Forest Meteorology 170:206-215.
Thudi, M., Palakurthi, R., Schnable, J.C., Chitikineni, A., Dreisigacker, S., Mace, E., et al. 2021. Genomic resources in plant breeding for sustainable agriculture. Journal of Plant Physiology 257:153351.
Tischer, C., Kirjavainen, P., Matterne, U., Tempes, J., Willeke, K., Keil, T., et al. 2022. Interplay between natural environment, human microbiota and immune system: A scoping review of interventions and future perspectives towards allergy prevention. Science of the Total Environment 821:153422.
Tu, A., Xie, S., Mo, M., Song, Y., Li, Y. 2021. Water budget components estimation for a mature citrus orchard of southern China based on HYDRUS-1D model. Agricultural Water Management 243:106426.
Vincent, H., Hole, D., Maxted, N. 2022. Congruence between global crop wild relative hotspots and biodiversity hotspots. Biological Conservation 265:109432.
Widrlechner, M.P., Daly, C., Keller, M., Kaplan, K. 2012. Horticultural applications of a newly revised USDA Plant Hardiness Zone Map. HortTechnology 22:6-19.
Wild, M., Behm, S., Beck, C., Cyrys, J., Schneider, A., Wolf, K., et al. 2022. Mapping the time-varying spatial heterogeneity of temperature processes over the urban landscape of Augsburg, Germany. Urban Climate 43:101160.
Xiang, J.W., Zhang, L.P., Deng, Y., She, D.X., Zhang, Q. 2021. Projection and evaluation of extreme temperature and precipitation in major regions of China by CMIP6 models. Engineering Journal of Wuhan University 54:46-57.
Xu, W., Du, Q., Yan, S., Cao, Y., Liu, X., Guan, D., et al. 2022. Geographical distribution of As-hyperaccumulator *Pteris vittata* in China: Environmental factors and climate changes. Science of the Total Environment 803:149864.

Yang, J., Huang, Y., Jiang, X., Chen, H., Liu, M., Wang, R. 2022. Potential geographical distribution of the endangered plant *Isoetes* under human activities using MaxEnt and GARP. Global Ecology and Conservation 38:e02186.
Yue, L., Cheng, Q.Q., Yang, Q. 2018. The resource survey of *Citri sarcodactylis* Fructus. Guangdong Chemical Industry 45:34-36.
Zhai, T., Wang, J., Fang, Y., Qin, Y., Huang, L., Chen, Y. 2020. Assessing ecological risks caused by human activities in rapid urbanization coastal areas: Towards an integrated approach to determining key areas of terrestrial-oceanic ecosystems preservation and restoration. Science of the Total Environment 708:135153.
Zhang, X., Xie, L., Long, J., Xie, Q., Zheng, Y., Liu, K., et al. 2021. Salidroside: A review of its recent advances in synthetic pathways and pharmacological properties. Chemico-Biological Interactions 339:109268.
Zhang, S.D., Yang, H.Y., Zeng, J., Li, M. 2018. Research progress on Citri Sarcodactylis Fructus. China Journal of Traditional Chinese Medicine and Pharmacy 33:3510-3514.
Zhao, X.L. 2012. Research progress of physiologically active compounds of bergamot. Science and Technology of Food Industry 33:393-399.
Zhao, W.L., Chen, H.G., Yuan, Y.Y., Zhang, J., Du, T., Jin, L. 2021. The impact of climate change on the distribution pattern of the suitable growing region for Tibetan medicine *Lamiophlomis rotata*. Acta Agrestia Sinica 29:956-964.
Zhao, Y.Y., Zhang, J.Y., Peng, T., He, P.Y., Kuang, Y. 2020. Comparative analysis of the components of volatile oil in *Citrus medica* from different producing areas. China Pharmacy 31:423-428.